JOURNAL OF GUIDANCE, CONTROL, AND DYNAMICS
Vol. 32, No. 6, November–December 2009

Engineering Notes

Nonlinear Hierarchical Flight Controller for Unmanned Rotorcraft: Design, Stability, and Experiments

Farid Kendoul*
Chiba University, Chiba City 263-8522, Japan

DOI: 10.2514/1.43768

I. Introduction

ALTHOUGH the research on unmanned aerial vehicles (UAVs) goes back to the last decade, the UAV control has a rich literature with different control techniques. Conventional approaches to UAV flight control involve dynamics linearization about a set of preselected equilibrium conditions or trim points. Then, many linear control techniques, such as proportional integral derivative or linear quadratic regulator controllers, can be applied. However, these approaches suffer from performance degradation when the aircraft moves away from a design trim point. Hence, gain scheduling is usually required to obtain acceptable performance. The main drawback of this approach is the severe tradeoff between control performance and the number of required trim points.

To overcome some of the limitations and drawbacks of the previous linear approaches, a variety of nonlinear flight control techniques have been developed. Among these, feedback linearization [1], model predictive control [2], dynamic inversion [3], adaptive control [4], robust control [5], backstepping [6], and nested saturation [7] techniques have received much of the attention and showed great promise. In actual flight and aerospace applications, the separate inner- and outer-loop approach is more commonly taken because it is usually simpler and results in good flight performance. In designing these practical controllers, the conventional conceptual separation between the position (outer loop) and the orientation (inner loop) is made. Most existing inner- and outer-loop controllers suffer from the lack of stability analysis and robustness with respect to model inversion errors and coupling terms. Our objective is to design a multiple-input/multiple-output nonlinear flight controller that performs well in practice while ensuring the asymptotic stability of the closed-loop system.

In this Note, we present the main steps for designing a hierarchical flight controller using the inner- and outer-loop control scheme. The proposed control system is based on the nonlinear model of rotorcraft UAVs and considers a system's nonlinearities as well as coupling between the rotational and translational dynamics. By exploiting its structural properties, the standard mathematical model of rotorcraft UAVs has been transformed into two cascaded linear subsystems that are coupled by a nonlinear interconnection term. Partial passivation design has been used to synthesize control laws for each subsystem, thereby resulting in an outer loop with slow dynamics that controls the position and an inner loop with fast dynamics that controls the orientation. The asymptotic stability of the entire connected system is proven by exploiting the theories of systems in cascade. The resulting nonlinear controller is thus easy to implement and tune, and it guarantees the asymptotic stability of the closed-loop system.

Received 12 February 2009; revision received 21 June 2009; accepted for publication 1 July 2009.

*Postdoctoral Research Fellow, Department of Electronics and Mechanical Engineering, Robotics and Control Laboratory; fkendoul@restaff.chiba-u.jp.

II. Nonlinear Hierarchical Controller: Design and Stability

The dynamics of small and lightweight rotorcraft UAVs such as the quadrotor helicopter can be represented by the following mathematical model [7,8], in which rotor dynamics, gyroscopic effects, and blade flapping can be neglected because they do not affect the overall dynamics of the system:

$$\begin{cases} \ddot{\xi} = \frac{1}{m} u R e_z - g e_z \\ M(\eta)\ddot{\eta} + C(\eta, \dot{\eta})\dot{\eta} = \Psi(\eta)^T \tau \end{cases} \tag{1}$$

$\xi = (x, y, z)$ and $\eta = (\phi, \theta, \psi)$ are the rotorcraft position and orientation, respectively. $u \in \mathbb{R}$ and $\tau \in \mathbb{R}^3$ are the applied thrust and torque vector. The body inertia matrix is denoted by $J \in \mathbb{R}^{3\times3}$ and the mass by $m \in \mathbb{R}$. The pseudoinertial matrix M is defined as $M(\eta) = \Psi(\eta)^T J \Psi(\eta)$, and the matrix C is given by $C(\eta, \dot{\eta}) = -\Psi(\eta)^T J \dot{\Psi}(\eta) + \Psi(\eta)^T sk(\Psi(\eta)\dot{\eta}) J \Psi(\eta)$. The sk operation is defined here from $\mathbb{R}^3$ to $\mathbb{R}^{3\times3}$, such that $sk(x)$ is a skew-symmetric matrix associated to the vector product $sk(x)y := x \times y$ for any vector $y \in \mathbb{R}^3$. $R \in \mathbb{R}^{3\times3}$ and $\Psi \in \mathbb{R}^{3\times3}$ are the rotation matrix and Euler matrix:

$$R = \begin{pmatrix} c\theta c\psi & s\phi s\theta c\psi - c\phi s\psi & c\phi s\theta c\psi + s\phi s\psi \\ c\theta s\psi & s\phi s\theta s\psi + c\phi c\psi & c\phi s\theta s\psi - s\phi c\psi \\ -s\theta & s\phi c\theta & c\phi c\theta \end{pmatrix}$$

and

$$\Psi(\eta) = \begin{pmatrix} 1 & 0 & -\sin\theta \\ 0 & \cos\phi & \cos\theta\sin\phi \\ 0 & -\sin\phi & \cos\theta\cos\phi \end{pmatrix}$$

where $s(x)$ and $c(x)$ are abbreviations for $\sin(x)$ and $\cos(x)$.

Controller design for nonlinear system (1), which is subject to strong coupling, offers both practical significance and theoretical challenges. In this Note, the control design for rotorcraft UAVs is addressed by transforming nonlinear model (1) into two linear systems coupled by a nonlinear term.

Because the attitude dynamics in Eq. (1) is a fully actuated mechanical system for $\theta \neq k\pi/2$, it is exact feedback linearizable. In fact, by considering the following change of variables

$$\tau = J\Psi(\eta)\tilde{\tau} + \Psi^{-1} C(\eta, \dot{\eta})\dot{\eta} \tag{2}$$

system (1) can be written in the following form:

$$\begin{cases} \ddot{x} = \frac{1}{m} u(\cos\phi\sin\theta\cos\psi + \sin\phi\sin\psi), & \ddot{\phi} = \tilde{\tau}_\phi \\ \ddot{y} = \frac{1}{m} u(\cos\phi\sin\theta\sin\psi - \sin\phi\cos\psi), & \ddot{\theta} = \tilde{\tau}_\theta \\ \ddot{z} = \frac{1}{m} u\cos\theta\cos\phi - g, & \ddot{\psi} = \tilde{\tau}_\psi \end{cases} \tag{3}$$

Now we apply the backstepping principle to transform system (3) into two subsystems in cascade. In contrast to the complexity of standard backstepping approaches, the control strategy considered in this Note is very simple and easy to implement and has been effective in a very broad range of aerospace applications.

Let us first define a virtual control vector $\mu \in \mathbb{R}^3$ as follows:

$$\mu = \mathfrak{f}(u, \phi_d, \theta_d, \psi_d) = \frac{1}{m} u R(\phi_d, \theta_d, \psi_d) e_z - g e_z \tag{4}$$

where $\mathfrak{f}(.)$: $\mathbb{R}^3 \to \mathbb{R}^3$ is a continuous invertible function. Physically, the control vector μ corresponds to the desired force vector. Its magnitude is the thrust u produced by the rotors, and its orientation is defined by the body attitude (ϕ, θ, ψ). ϕ_d, θ_d, and ψ_d in Eq. (4) are thus the desired roll, pitch, and yaw angles.

By recalling Eq. (4), the components of μ are given by

$$\begin{cases} \mu_x = \frac{1}{m}u(\cos\phi_d \sin\theta_d \cos\psi_d + \sin\phi_d \sin\psi_d) \\ \mu_y = \frac{1}{m}u(\cos\phi_d \sin\theta_d \sin\psi_d - \sin\phi_d \cos\psi_d) \\ \mu_z = \frac{1}{m}u\cos\theta_d \cos\phi_d - g \end{cases} \tag{5}$$

where (μ_x, μ_y, μ_z) are the force vector components along the X–Y–Z axes that are needed for tracking some reference position trajectory. These desired control inputs are computed by the outer-loop controller. They are then used to compute the desired force vector magnitude and orientation, $(u, \phi_d, \theta_d) = \mathfrak{f}^{-1}(\mu_x, \mu_y, \mu_z)$, that is,

$$\begin{cases} u = m\sqrt{\mu_x^2 + \mu_y^2 + (\mu_z + g)^2} \\ \phi_d = \sin^{-1}(m\frac{\mu_x \sin\psi_d - \mu_y \cos\psi_d}{u}) \\ \theta_d = \tan^{-1}(\frac{\mu_x \cos\psi_d + \mu_y \sin\psi_d}{\mu_z + g}) \end{cases} \tag{6}$$

The desired yaw angle ψ_d is given by the user or by some high-level guidance system.

Because the desired angles $(\phi_d, \theta_d, \psi_d)$ are the outputs of the orientation subsystem, they cannot be assigned or provided instantaneously. They are thus considered as reference trajectories for the inner-loop controller. Therefore, we define the following attitude error vector $e = (e_\eta, e_{\dot\eta})^T \in R^6$ such that $e_\eta = \eta - \eta_d$ and $e_{\dot\eta} = \dot\eta - \dot\eta_d$.

Now, by replacing (ϕ, θ, ψ) in Eq. (3) with $(\phi_d + e_\phi, \theta_d + e_\theta, \psi_d + e_\psi)$ and exploiting some useful relations between trigonometric functions, such as

$$\begin{cases} \sin(a+b) = \sin(a) + \sin(b/2)\cos(a + b/2) \\ \cos(a+b) = \cos(a) - \sin(b/2)\sin(a + b/2) \end{cases} \tag{7}$$

the rotorcraft translational dynamics (3) can be written in the following form:

$$\begin{cases} \ddot{x} = \frac{1}{m}u[(\cos\phi_d \sin\theta_d \cos\psi_d + \sin\phi_d \sin\psi_d) + h_x(\phi_d, \theta_d, \psi_d, e_\phi, e_\theta, e_\psi)] = \mu_x + \frac{1}{m}uh_x(.) \\ \ddot{y} = \frac{1}{m}u[(\cos\phi_d \sin\theta_d \sin\psi_d - \sin\phi_d \cos\psi_d) + h_y(\phi_d, \theta_d, \psi_d, e_\phi, e_\theta, e_\psi)] = \mu_y + \frac{1}{m}uh_y(.) \\ \ddot{z} = \frac{1}{m}u[\cos\theta_d \cos\phi_d + h_z(\phi_d, \theta_d, e_\phi, e_\theta)] - g = \mu_z + \frac{1}{m}uh_z(.) \end{cases} \tag{8}$$

The components of the interconnection vector $h(\phi_d, \theta_d, \psi_d, e_\phi, e_\theta, e_\psi) \in \mathbb{R}^3$ are composed of the multiplication and summation of sin(.) and cos(.) functions.

By defining the position-velocity tracking error $\chi = (\xi - \xi_d, \upsilon - \upsilon_d)^T \in \mathbb{R}^6$ and recalling Eqs. (3) and (8), we can write

$$\begin{cases} \dot\chi = \underbrace{A_1\chi + B_1(\mu - \ddot\xi_d)}_{f(\chi, \mu, \ddot\xi_d)} + \underbrace{\frac{1}{m}uH(\eta_d, e_\eta)}_{\Delta(u, \eta_d, e_\eta)} \\ \dot e = A_2 e + B_2(\tilde\tau - \ddot\eta_d) \end{cases} \tag{9}$$

where $H(\eta_d, e_\eta) = (0, 0, 0, h_x, h_y, h_z)^T$. The matrices $A_1 \in \mathbb{R}^{6\times6}$, $B_1 \in \mathbb{R}^{6\times3}$, $A_2 \in \mathbb{R}^{6\times6}$, and $B_2 \in \mathbb{R}^{6\times3}$ are defined as follows:

$$A_1 = A_2 = \begin{bmatrix} 0 & 0 & 0 & 1 & 0 & 0 \\ 0 & 0 & 0 & 0 & 1 & 0 \\ 0 & 0 & 0 & 0 & 0 & 1 \\ 0 & 0 & 0 & 0 & 0 & 0 \\ 0 & 0 & 0 & 0 & 0 & 0 \\ 0 & 0 & 0 & 0 & 0 & 0 \end{bmatrix}, \quad B_1 = B_2 = \begin{bmatrix} 0 & 0 & 0 \\ 0 & 0 & 0 \\ 0 & 0 & 0 \\ 1 & 0 & 0 \\ 0 & 1 & 0 \\ 0 & 0 & 1 \end{bmatrix} \tag{10}$$

The rotorcraft control problem is thus formulated as the control of two linear subsystems that are coupled by a nonlinear term $\Delta(u, \eta_d, e_\eta)$. It can be controlled using partial or full passivation design [9].

In partial-state feedback designs such as the one used here, the two linear subsystems are controlled independently ($\mu = \alpha(\chi, \ddot\xi_d)$ and $\tilde\tau = \beta(e, \ddot\eta_d)$). The problem is thus to stabilize the e subsystem without destroying the global asymptotic stability (GAS) property of the χ subsystem. In this case, the interconnection term $\Delta(u, \eta_d, e_\eta)$ acts as a disturbance on the χ subsystem and must be driven to zero. Such partial-state feedback designs are of interest because of their simplicity, especially for implementation on physical systems. However, it is difficult to prove the GAS property for the entire connected system.

In full-state feedback designs, the interconnection term plays an active role in controlling the χ subsystem. In this case, the orientation error e in Eq. (9) is treated as an additional input for the χ subsystem. This results in a relatively simple stability analysis, but at the expense of the control law complexity.

In this Note, we consider the partial-state feedback design. The control objective is thus to synthesize the control laws $\mu(\chi, \ddot\xi_d)$ and $\tilde\tau(e, \ddot\eta_d)$ such that the tracking errors χ and e will asymptotically converge to zero.

A. Control and Stability of Systems in Cascade

The idea behind the inner–outer-loop control scheme is to design two independent controllers for the χ and e subsystems without considering the interconnection term $\Delta(u, \eta_d, e_\eta)$. As mentioned in the Introduction, this procedure simplifies the control design and results in simple and efficient control laws. However, the stability of the connected closed-loop system and its robustness with respect to $\Delta(u, \eta_d, e_\eta)$ have not been proven. Therefore, the main contribution of this Note is the analysis of the controller stability and robustness with respect to the interconnection and coupling term $\Delta(u, \eta_d, e_\eta)$.

Much work has been done on the stability analysis of systems in cascade [9,10]. One of the most important theorems on the stability of systems in cascade is the following theorem expressed by Sontag [10].

Theorem 1: If there is a feedback $\mu = \alpha(\chi, \ddot\xi_d)$ such that $\chi = 0$ is an asymptotically stable equilibrium of $\dot\chi = f(\chi, \alpha(\chi, \ddot\xi_d))$, then any partial-state feedback control $\tilde\tau = \beta(e, \ddot\eta_d)$ that renders the e subsystem equilibrium $e = 0$ asymptotically stable also achieves asymptotic stability of $(\chi, e) = (0, 0)$. Furthermore, if the two subsystems are both GAS, then, as $t \to \infty$, every solution $(\chi(t), e(t))$ either converges to $(\chi, e) = (0, 0)$ (GAS) or is unbounded.

Therefore, the stability of the connected system (9) will be ensured if we choose stabilizing feedbacks $\mu = \alpha(\chi, \ddot\xi_d)$ and $\tilde\tau = \beta(e, \ddot\eta_d)$ and prove that all the trajectories $(\chi(t), e(t))$ are bounded.

One of the major tools usually used to show the boundedness of connected system trajectories is the input-to-state-stability (ISS) property [10]. The ISS property is a strong condition that is often difficult to verify. Indeed, the verification of the ISS property for system (9) is very difficult due to the complexity of the interconnection term $\Delta(u, \eta_d, e_\eta)$. Consequently, we propose a theorem that guarantees the GAS of the connected system (9) provided that the interconnection term $\Delta(u, \eta_d, e_\eta)$ satisfies some relaxed conditions. This theorem is inspired by Theorem 4.7 on page 129 of Sepulcre et al. [9].

Theorem 2: Let $\mu = \alpha(\chi, \ddot{\xi}_d)$ be a stabilizing feedback for the nonconnected subsystem $\dot{\chi} = f(\chi, \mu, \ddot{\xi}_d)$. Let $\tilde{\tau} = \beta(e, \ddot{\eta}_d)$ be any C^1 partial-state feedback such that the equilibrium point $e = 0$ is GAS and locally exponentially stable (LES). Suppose that there exist a positive constant c_1 and one class-$\mathcal{K}$ function $\gamma(.)$, differentiable at $e = 0$, such that

$$\|\Delta(\chi, e_\eta)\| \leq \gamma(\|e_\eta\|)\|\chi\| \quad \text{for } \|\chi\| \geq c_1 \tag{11}$$

If there exist a positive semidefinite radially unbounded function $V(\chi)$ and positive constants c_2 and c_3 such that, for $\|\chi\| \geq c_2$,

$$\begin{cases} \frac{\partial V}{\partial \chi} f(\chi, \alpha(\chi, \ddot{\xi}_d)) \leq 0 \\ \|\frac{\partial V}{\partial \chi}\|\|\chi\| \leq c_3 V(\chi) \end{cases} \tag{12}$$

then the feedbacks $\mu = \alpha(\chi, \ddot{\xi}_d)$ and $\tilde{\tau} = \beta(e, \ddot{\eta}_d)$ guarantee the boundedness of all the solutions of Eq. (9). Furthermore, if $\dot{\chi} = f(\chi, \alpha(\chi, \ddot{\xi}_d))$ is GAS, then the equilibrium point $(\chi, e) = (0, 0)$ is GAS.

Proof: The proof of Theorem 2 is given in the Appendix.

B. Control Law Synthesis and Closed-Loop System Stability Analysis

Here, we apply Theorems 1 and 2 to synthesize two control laws for the UAV transformed model given by Eq. (9). Theorem 2 is used to prove the asymptotic stability of the connected closed-loop system. The control design can thus be achieved in three steps:

1) Choose the control law $\mu = \alpha(\chi, \ddot{\xi}_d)$ that guarantees the global exponential stability (GES) of the χ subsystem without the interconnection term $\Delta(\chi, e_\eta)$.

2) Choose the feedback $\tilde{\tau} = \beta(e, \ddot{\eta}_d)$ such that the e subsystem is GES.

3) Prove that system (9) satisfies the conditions stated in Theorem 2. In fact, we need to prove that the interconnection term $\Delta(\chi, e_\eta)$ satisfies growth condition (11).

Because the χ and e subsystems are linear, we can use simple linear controllers such as proportional derivative or proportional integral derivative. Therefore, we synthesize two intermediary control laws

$$\begin{cases} \mu = -K_\chi \chi + \ddot{\xi}_d, & K_\chi \in \mathbb{R}^{3\times 6} \\ \tilde{\tau} = -K_e e + \ddot{\eta}_d, & K_e \in \mathbb{R}^{3\times 6} \end{cases} \tag{13}$$

such that the matrices $A_\chi = A_1 - B_1 K_\chi$ and $A_e = A_2 - B_2 K_e$ are Hurwitz.

By substituting Eq. (13) into Eq. (9), the closed-loop system is given by

$$\begin{cases} \dot{\chi} = A_\chi \chi + \Delta(\chi, e_\eta) \\ \dot{e} = A_e e \end{cases} \tag{14}$$

Although A_χ and A_e are Hurwitz, the asymptotic stability of closed-loop system (14) cannot be directly deduced because of the interconnection term $\Delta(\chi, e_\eta)$. Thus, we apply Theorem 2 to prove the asymptotic stability of connected closed-loop system (14).

Because A_χ and A_e are Hurwitz, the χ (without the interconnection term) and e subsystems are GES, which is stronger than the GAS property. The GES of the χ subsystem implies that there exist a positive definite radially unbounded function $V(\chi)$ and positive constants c_2 and c_3 such that, for $\|\chi\| \geq c_2$, $\frac{\partial V}{\partial \chi} A_\chi \chi \leq 0$ and $\|\frac{\partial V}{\partial \chi}\|\|\chi\| \leq c_3 V(\chi)$. Therefore, condition (12) of Theorem 2 is satisfied.

Now it remains to be shown that the interconnection term $\Delta(\chi, e_\eta)$ satisfies growth restriction (11) of Theorem 2, and this is the most difficult part.

The norm of the interconnection term $\Delta(\chi, e_\eta)$ can be expressed as follows:

$$\|\Delta(\chi, e_\eta)\| = \tfrac{1}{m}|u(\chi)|\|H(\chi, e_\eta)\| = \tfrac{1}{m}|u(\chi)|\sqrt{h_x^2 + h_y^2 + h_z^2} \tag{15}$$

where

$$|u(\chi)| = m\|\mu(\chi) + g e_z\| = m\sqrt{\mu_x^2 + \mu_y^2 + (\mu_z + g)^2}$$

Before proving the boundedness of the interconnection term $\Delta(\chi, e_\eta)$, we need the following two Lemmas.

Lemma 1: Assume that the desired trajectories $\xi_d(t) = (x_d(t), y_d(t), z_d(t))$ and their time derivatives are bounded and $L_d = \|\ddot{\xi}_d\|_\infty$. Then, there exist positive constants r and k_1 such that the collective thrust feedback $u(\chi)$ satisfies the following properties:

$$|u(\chi)| \leq \begin{cases} k_1\|\chi\|, & \text{for } \|\chi\| \geq r \\ k_1 r, & \text{for } \|\chi\| < r \end{cases} \tag{16}$$

Lemma 2: There exists a positive constant k_2 such that the coupling term $H(\chi, e_\eta)$ satisfies the following inequality:

$$\|H(\chi, e_\eta)\| \leq k_2\|e_\eta\| \tag{17}$$

The proofs of Lemmas 1 and 2 are given in the Appendix.

From Lemmas 1 and 2, we can write that, for $\|\chi\| \geq r$, we have

$$\|uH(.)\| \leq k_1\|\chi\|k_2\|e_\eta\| = k\|e_\eta\|\|\chi\| \tag{18}$$

where $k = k_1 k_2$ is a positive constant.

Finally, we obtain the following inequality:

$$\|\Delta(\chi, e_\eta)\| = \tfrac{1}{m}\|uH\| \leq \gamma(\|e_\eta\|)\|\chi\|, \quad \text{for } \|\chi\| \geq r \tag{19}$$

where $\gamma(e_\eta) = \frac{k}{m}\|e_\eta\|$ is a class-$\mathcal{K}$ function.

Thus, all the conditions of Theorems 1 and 2 are satisfied and the GAS of the equilibrium point $(\chi, e) = (0, 0)$ is then guaranteed.

Remark 1: The final control inputs $u \in \mathbb{R}$ (thrust) and $\tau \in \mathbb{R}^3$ (torque) are computed using Eqs. (2) and (6) and they are expressed as follows:

$$\begin{cases} u = m\|\mu(\chi, \ddot{\xi}_d) + g e_z\| = m\|-K_\chi \chi + \ddot{\xi}_d + g e_z\| \\ \tau = J\Psi(\eta)\tilde{\tau} + \Psi^{-1}C(\eta, \dot{\eta})\dot{\eta} = J\Psi(\eta)(-K_e e + \ddot{\eta}_d) + \Psi^{-1}C(\eta, \dot{\eta})\dot{\eta} \end{cases} \tag{20}$$

The block diagram of the overall controller is shown in Fig. 1.

III. Flight Tests and Experimental Results

To evaluate the performance of the proposed nonlinear controller, we have built a miniature (700 g) aerial platform [11] with onboard microprocessor and navigation sensors, and we have performed real-time flight tests with various mission scenarios. Here, we demonstrate the ability of the developed control system to achieve accurate waypoint navigation and perform automatic takeoff, trajectory tracking, hovering, and automated landing. In this test, a set of four waypoints were chosen and desired trajectories $(\xi_d(t), \upsilon_d(t), \psi_d(t))$ were generated in real time by the guidance system [11].

In Fig. 2, we can clearly observe that the rotorcraft passed successfully through all the waypoints. The real trajectories are almost identical to the reference trajectories, thereby demonstrating the good performance of the proposed controller. From Fig. 2c, we can also see that, despite low-cost sensors, we have achieved an accurate height control (± 1.5 m) even during relatively high-speed flight (5 m/s).

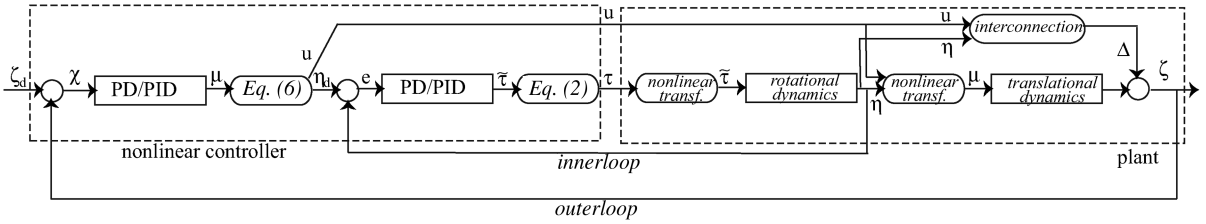

Fig. 1 Block diagram of the interconnected system and controller.

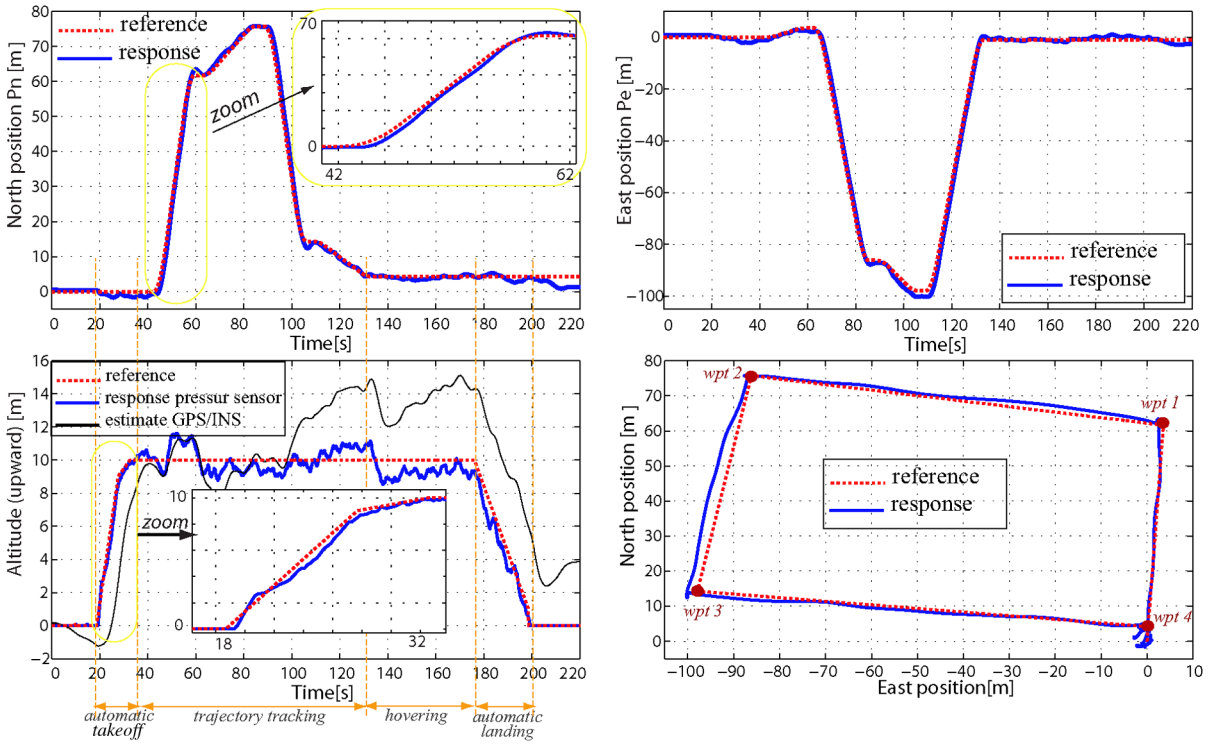

Fig. 2 Trajectory tracking during waypoint navigation.

IV. Conclusions

We have described the design of a practical nonlinear controller that exploits the model structure of rotorcraft unmanned aerial vehicles. The asymptotic stability property has been proven for the connected closed-loop system, and the performance of the proposed flight controller has been evaluated in real-time flight tests. We have also demonstrated the ability to provide effective waypoint navigation and trajectory tracking capabilities to small and low-cost systems such as the mini quadrotor helicopter.

Appendix: Proofs

I. Proof of Theorem 2

Let $(\chi(0), e(0))$ be an arbitrary initial condition, and let $V(\chi)$ be a semidefinite positive function. By recalling Eqs. (11) and (12), then for $\|\chi\| \geq \max(c_1, c_2)$ we have the following inequalities:

$$\dot{V}(\chi) = \underbrace{\frac{\partial V}{\partial \chi} f(.)}_{\leq 0} + \frac{\partial V}{\partial \chi}\Delta(.) \leq \frac{\partial V}{\partial \chi}\Delta(.) \leq \left\|\frac{\partial V}{\partial \chi}\right\| \|\Delta\| \leq$$

$$\left\|\frac{\partial V}{\partial \chi}\right\| \gamma(\|e_\eta\|)\|\chi\| \leq c_3 V(\chi)\gamma(\|e_\eta\|) \tag{A1}$$

Because the equilibrium point $e_\eta = 0$ is GAS and LES, then $\|e_\eta\|$ converges to zero exponentially. This implies that

$$\gamma(\|e_\eta(t)\|) \leq \gamma(\|e_\eta(0)e^{-at}\|) \leq \gamma_1(\|e_\eta(0)\|)e^{-at}$$

where a is a positive constant and $\gamma_1(.)$ is a class-$\mathcal{K}$ function.

Now, the derivative of $V(\chi)$ satisfies

$$\dot{V}(\chi) \leq c_3 V(\chi)\gamma_1(\|e_\eta(0)\|)e^{-at}, \quad \text{for } \|\chi\| \geq \max(c_1, c_2)$$

We define a positive constant as $c = c_3\gamma_1(\|e_\eta(0)\|)$. Thus,

$$\dot{V}(\chi) \leq cV(\chi)e^{-at}, \quad \text{for } \|\chi\| \geq \max(c_1, c_2)$$

This relation proves the boundedness of $V(\chi)$ because

$$V(\chi) \leq V(\chi(0))e^{\int_0^t ce^{-as}\,ds} \leq \gamma_2(\|e_\eta(0)\|)V(\chi(0))$$

for some $\gamma_2(.) \in \mathcal{K}$.

Because $V(\chi)$ is radially unbounded, the boundedness of $V(\chi)$ implies the boundedness of $\|\chi\|$.

Therefore, the GAS of the equilibrium point $(\chi, e) = (0, 0)$ follows from Theorem 1.

II. Proofs of Lemmas 1 and 2

Boundedness of $|u(\chi)|$: Let us recall the expressions of the thrust u and the feedback μ.

$$\begin{cases} |u(\chi)| = m\|\mu(\chi, \ddot{\xi}_d) + ge_3\| \\ \mu(\chi, \ddot{\xi}_d) = -K_\xi\chi_\xi - K_\upsilon\chi_\upsilon + \ddot{\xi}_d \end{cases} \tag{A2}$$

Let $\lambda_\xi > 0$ and $\lambda_\upsilon > 0$ be the maximum values of the K_ξ and K_υ eigenvalues, respectively. Thus, we write

$$
\begin{aligned}
|u(\chi)| &= m\|ge_3 + \ddot{\xi}_d - K_\xi\chi_\xi - K_\upsilon\chi_\upsilon\| \\
&\le m(g + \|\ddot{\xi}_d\| + \lambda_\xi\|\chi_\xi\| + \lambda_\upsilon\|\chi_\upsilon\|) \\
&\le m(g + L_d + \max(\lambda_\xi, \lambda_\upsilon)(\|\chi_\xi\| + \|\chi_\upsilon\|)) \\
&\le m(g + L_d) + m\max(\lambda_\xi, \lambda_\upsilon)\sqrt{2}\|\chi\|
\end{aligned}
$$

because

$$
\begin{aligned}
(\|\chi_\xi\| + \|\chi_\upsilon\|)^2 &= \|\chi_\xi\|^2 + \|\chi_\upsilon\|^2 + 2\|\chi_\xi\|\|\chi_\upsilon\| \\
&\le 2(\|\chi_\xi\|^2 + \|\chi_\upsilon\|^2)
\end{aligned}
$$

which implies that

$$
\|\chi_\xi\| + \|\chi_\upsilon\| \le \sqrt{2}\sqrt{\|\chi_\xi\|^2 + \|\chi_\upsilon\|^2} = \sqrt{2}\|\chi\|
$$

Setting $c \triangleq m\sqrt{2}\max(\lambda_\xi, \lambda_\upsilon)$, we get

$$
\begin{aligned}
|u(\chi)| &\le m(g + L_d) + c\|\chi\| \le c\left(\frac{mg + mL_d}{c} + \|\chi\|\right) \\
&\le c(r + \|\chi\|), \\
\text{where } r &= \frac{mg + mL_d}{c}
\end{aligned}
$$

From these inequalities, we deduce that

$$
|u(\chi)| \le \begin{cases} k_1\|\chi\|, & \text{for all } \|\chi\| \ge r \\ k_1 r, & \text{for all } \|\chi\| < r \end{cases} \tag{A3}
$$

where $k_1 = 2c$.

Boundedness of $\|H(.)\|$: We had $\|H(\chi, e_\eta)\| = \sqrt{h_x^2 + h_y^2 + h_z^2}$, where the components (h_x, h_y, h_z) are functions of sin(arg) and cos(arg). The argument arg may be ϕ_d, $e_\phi/2$, $\phi_d + e_\phi/2$, θ_d, $e_\theta/2$, $\theta_d + e_\theta/2$, ψ_d, $e_\psi/2$, and $\psi_d + e_\psi/2$.

Let us recall some trivial inequalities that are exploited to prove the boundedness of $\|H(\chi, e_\eta)\|$:

$$
\begin{aligned}
&|\sin a| \le |a|, \qquad |\sin a| \le 1 \quad \text{and} \quad |\cos a| \le 1 \\
&|a||b| \le \frac{1}{2}(|a| + |b|), \quad \text{for } |a| \le 1 \quad \text{and} \quad |b| \le 1 \\
&|a||b||c| \le \frac{1}{2}(|a| + |b| + |c|), \quad \text{for } |a| \le 1 \\
&\qquad |b| \le 1 \quad \text{and} \quad |c| \le 1
\end{aligned} \tag{A4}
$$

By writing the exact expressions of (h_x, h_y, h_z) and doing some mathematical calculations, it is possible to show that

$$
\begin{aligned}
|h_x| &\le c_1(|e_\theta| + |e_\phi| + |e_\psi|), \qquad h_x^2 \le c_4(e_\theta^2 + e_\phi^2 + e_\psi^2) \\
|h_y| &\le c_2(|e_\theta| + |e_\phi| + |e_\psi|), \qquad h_y^2 \le c_5(e_\theta^2 + e_\phi^2 + e_\psi^2) \\
|h_z| &\le c_3(|e_\theta| + |e_\phi|), \qquad h_z^2 \le c_6(e_\theta^2 + e_\phi^2)
\end{aligned} \tag{A5}
$$

where c_1, c_2, c_3, c_4, c_5, and c_6 are positive constants.

Proof: We will now show that the component h_z verifies the inequalities in Eq. (A5). By following the same steps, it is easy to show that the other components h_x and h_y also satisfy the inequalities in Eq. (A5).

Let us first write the exact expression of h_z, which is given by

$$
\begin{aligned}
h_z &= \cos\phi_d[-\sin(e_\theta/2)\sin(\theta_d + e_\theta/2)] \\
&\quad + \cos\theta_d[-\sin(e_\phi/2)\sin(\phi_d + e_\phi/2)] \\
&\quad + [-\sin(e_\theta/2)\sin(\theta_d + e_\theta/2)][-\sin(e_\phi/2)\sin(\phi_d + e_\phi/2)]
\end{aligned} \tag{A6}
$$

By using inequalities in Eq. (A4) and keeping only the $\sin(e_\theta/2)$ and $\sin(e_\phi/2)$ terms, one can write

$$
\begin{aligned}
|h_z| &\le |\sin(e_\theta/2)| + |\sin(e_\phi/2)| + |\sin(e_\phi/2)||\sin(e_\theta/2)| \\
&\le \tfrac{3}{2}(|\sin(e_\theta/2)| + |\sin(e_\phi/2)|) \le \tfrac{3}{4}(|e_\theta| + |e_\phi|) \\
&\le c_3(|e_\theta| + |e_\phi|), \quad \text{with} \quad c_3 = \tfrac{3}{4}
\end{aligned} \tag{A7}
$$

By computing the square of the previous function and considering that $2|e_\theta||e_\phi| \le e_\theta^2 + e_\phi^2$, one can write

$$
h_z^2 \le c_3^2(e_\theta^2 + e_\phi^2 + 2|e_\theta||e_\phi|) \le 2c_3^2(e_\theta^2 + e_\phi^2) \le c_6(e_\theta^2 + e_\phi^2)
$$
$$
\text{with} \quad c_6 = 2c_3^2 = \tfrac{9}{8}
$$

After some mathematical developments, we can prove that the norm of the interconnection term $H(.)$ verifies the following inequalities:

$$
\begin{aligned}
\|H(\chi, e_\eta)\| &= \sqrt{h_x^2 + h_y^2 + h_z^2} \\
&\le \sqrt{c_4(e_\theta^2 + e_\phi^2 + e_\psi^2) + c_5(e_\theta^2 + e_\phi^2 + e_\psi^2) + c_6(e_\theta^2 + e_\phi^2)} \\
&\le \sqrt{(c_4 + c_5 + c_6)e_\theta^2 + (c_4 + c_5 + c_6)e_\phi^2 + (c_4 + c_5)e_\psi^2} \\
&\le \sqrt{(c_4 + c_5 + c_6)e_\theta^2 + (c_4 + c_5 + c_6)e_\phi^2 + (c_4 + c_5 + c_6)e_\psi^2} \\
&\le k\|e_\eta\| \quad \text{with} \quad k = \sqrt{c_4 + c_5 + c_6}
\end{aligned} \tag{A8}
$$

and this ends the Proof.

References

[1] Koo, T., and Sastry, S., "Output Tracking Control Design of a Helicopter Model Based on Approximate Linearization," *Proceedings of the IEEE Conference on Decision and Control*, Institute of Electrical and Electronics Engineers, New York, Dec. 1998, pp. 3635–3640.

[2] Shim, D. H., Kim, H. J., and Sastry, S., "A Flight Control System for Aerial Robots: Algorithms and Experiments," *Control Engineering Practice*, Vol. 11, No. 12, 2003, pp. 1389–1400. doi:10.1016/S0967-0661(03)00100-X

[3] Reiner, J., Balas, G., and Garrard, W., "Robust Dynamic Inversion for Control of Highly Maneuverable Aircraft," *Journal of Guidance, Control, and Dynamics*, Vol. 18, No. 1, 1995, pp. 18–24. doi:10.2514/3.56651

[4] Johnson, E., and Kannan, S., "Adaptive Trajectory Control for Autonomous Helicopters," *Journal of Guidance, Control, and Dynamics*, Vol. 28, No. 3, May–June 2005, pp. 524–538. doi:10.2514/1.6271

[5] La Civita, M., Papageorgiou, G., Messner, W. C., and Kanade, T., "Design and Flight Testing of an H_∞ Controller for a Robotic Helicopter," *Journal of Guidance, Control, and Dynamics*, Vol. 29, No. 2, April 2006, pp. 485–494. doi:10.2514/1.15796

[6] Bouabdallah, S., and Siegwart, R., "Backstepping and Sliding-Mode Techniques Applied to an Indoor Micro Quadrotor," *Proceedings of the IEEE International Conference on Robotics and Automation*, Institute of Electrical and Electronics Engineers, New York, April 2005, pp. 2247–2252.

[7] Kendoul, F., Lara, D., Fantoni, I., and Lozano, R., "Real-Time Nonlinear Embedded Control for an Autonomous Quad-Rotor Helicopter," *Journal of Guidance, Control, and Dynamics*, Vol. 30, No. 4, 2007, pp. 1049–1061. doi:10.2514/1.27882

[8] Olfati-Saber, R., "Nonlinear Control of Underactuated Mechanical Systems with Application to Robotics and Aerospace Vehicles," Ph.D. Thesis, Dept. of Electrical Engineering and Computer Science, Massachusetts Institute of Technology, Cambridge, MA, 2001.

[9] Sepulcre, R., Jankovic, M., and Kokotovic, P., *Constructive Nonlinear Control*, Communications and Control Engineering Series, Springer–Verlag, Berlin/New York/Heidelberg, 1997.

[10] Sontag, E., "Smooth Stabilization Implies Coprime Factorization," *IEEE Transactions on Automatic Control*, Vol. 34, No. 4, 1989, pp. 435–443. doi:10.1109/9.28018

[11] Kendoul, F., Zhenyu, Y., and Nonami, K., "Embedded Autopilot for Accurate Waypoint Navigation and Trajectory Tracking: Application to Miniature Rotorcraft UAVs," *Proceedings of the IEEE International Conference on Robotics and Automation*, Institute of Electrical and Electronics Engineers, New York, May 2009, pp. 2884–2890.